Geomorphology 443 (2023) 108934

Contents lists available at ScienceDirect

Geomorphology

journal homepage: www.journals.elsevier.com/geomorphology

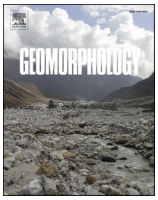

Polygons with halite-crusted floors and gypsum-raised rims in western Qaidam Basin and implications for polygonal landforms on Mars

Jiaming Zhu [a], Bo Wu [a,*], Tianlei Zhao [b], Yiliang Li [c,*]

[a] Planetary Remote Sensing Laboratory, Department of Land Surveying and Geo-Informatics, The Hong Kong Polytechnic University, Hung Hom, Kowloon, Hong Kong
[b] CAS Key Laboratory of Crust-Mantle Materials and Environments, School of Earth and Space Sciences, University of Science and Technology of China, Hefei 230026, China
[c] Department of Earth Sciences, The University of Hong Kong, Pokfulam Road, Hong Kong

ARTICLE INFO

Keywords:
Polygons
Qaidam Basin
Subsurface pore fluid
Halite crust
Gypsum made raised rim

ABSTRACT

Polygons ranging in size from a few meters to kilometers have been observed in playa fields on Earth and Mars. The historically hyperarid climate of the Qaidam Basin has allowed the development of extensive polygonal landforms with diverse geometric and genetic types. Here we report a terrain of polygons with a pan-like structure, raised rims, and a size of about 60 to 120 m, and spatial variation in mineral composition and geometry from the Dalangtan area of the western Qaidam Basin on the Tibetan Plateau. Spatially, the polygons in the northeastern part of the study area have complete rims, while the polygons in the southwest have incomplete rims. These polygons consist of a halite crust in the subsurface and raised rims formed mainly of gypsum. In some areas, the polygonal rims are broadened and form boundary belts that are up to ~30 m wide and about 1.2 m high. We suggest that the formation of the halite crust in the subsurface redirects upward migration of evaporitic pore fluids that accumulate gypsum deposits to form the wide polygonal boundary belts. We argue that the similarly sized polygons with raised rims on Mars have similar lateral and vertical structures caused successively by the strong evaporation of lacustrine brines and subsurface pore fluids.

1. Introduction

Polygonal landforms are common in arid regions on Earth. Numerous studies have examined the morphology and formation mechanisms of these polygons to understand climate evolution (El-Maarry et al., 2015; Krinsley, 1970; Neal et al., 1968; Tucker, 1981; Weinberger, 1999). In large basin playas, clay mass dehydration and the decline of the water table lead to shrinkage and subsequent formation of polygonal mud fissures (El-Maarry et al., 2015; Neal et al., 1968). Tucker (1981) established a thermal contraction model based on the formation of polygonal fissures in the Cheshire–Shropshire Basin. In the stratified muddy sedimentary area, dry mud fractures originate at the bottom and extend laterally to form a polygonal structure (Weinberger, 1999). Tucker (1981) suggests that some polygons with raised rims are formed when wind or water deposits clastic material to fill the fissures. Lokier (2012) concludes that the subtle topography of the underlying sediment controls the lateral displacement of the halite crust to produce the raised rim of the polygons. In an arid climate, intense evaporation and the growth of successive salt crystals can compress the mud surface and produce polygonal rims (Krinsley, 1970). Thermal contraction in permafrost forms fractures and gradually shapes vertical ice wedges with the seasonal freeze-thaw cycles on Earth (Lachenbruch, 1962), while allowing contraction of sand-filled cracks in sand-wedge polygons (Marchant et al., 2002; Marchant and Head III, 2007).

The Qaidam Basin is located in the west of Qinghai Province, on the northern edge of the Qinghai–Tibet Plateau in China. It is a large intermontane basin with a floor area of $>1.2 \times 10^5$ km^2. A growing number of reports describe this basin as a large martian analog in terms of geomorphology, climate, surface deposition, and microbial habitability (Anglés and Li, 2017; Cheng et al., 2017; Cheng et al., 2021; Dang et al., 2018; Kong et al., 2014; Xiao et al., 2017). The average elevation of the basin floor is about 2800 m, while the surrounding mountains have maximum elevations of over 5000 m (Chen and Bowler, 1986; Kapp et al., 2011; Meyer et al., 1998). These mountains serve as an effective topographic barrier, resulting in annual precipitation of <20 mm and annual evaporation of up to 2590 mm in the northwestern Qaidam Basin (Kong et al., 2018). A long, arid climatic trend that began about 25,000 years ago is causing a climatic transition from relatively

* Corresponding authors.
E-mail addresses: bo.wu@polyu.edu.hk (B. Wu), yiliang@hku.hk (Y. Li).

https://doi.org/10.1016/j.geomorph.2023.108934
Received 21 December 2022; Received in revised form 6 October 2023; Accepted 10 October 2023
Available online 11 October 2023

wet to dry in the Qaidam Basin (Chen and Bowler, 1986), resulting in a climatic environment characterized by numerous lacustrine landforms and massive salt deposits (Xiao et al., 2017).

The mineral composition of the playa sediments possibly controls the formation of polygons of different sizes in the western Qaidam Basin (Dang et al., 2018), although the giant polygon found in the northern plains of Mars may also be due to tectonic deformation (Pechmann, 1980). Based on Dang et al. (2018) and McGill and Hills (1992), we classified the size of the polygons into four groups: small (<10 m), medium (10–100 m), large (100–300 m), and giant (>300 m). Dang et al. (2018) reported that in the Dalangtan Playa polygonal terrain, halite is the most abundant material, especially in the fields of small polygonal rims, while clay minerals (illite and chlorite) are generally abundant in the fields of medium and large polygonal rims. Relatively high gypsum contents are found in the fields of the large polygons in southwestern Dalangtan Playa (Dang et al., 2018). Dang et al. (2018) suggest that the polygons with raised rims were formed by evaporative halite growth. In addition, the formation of the unique "jigsaw puzzle" polygons (JPPs) is due to changes in the composition of sulfate minerals, particularly, volume expansion from the transformation of thenardite to gypsum (Cheng et al., 2021). Both sulfate and halite are abundant in large polygons with raised rims (Dang et al., 2018), but no study has examined the combined effect of halite and sulfates on the formation of such polygons on Earth and Mars.

Here, we report a terrain with pan-like, raised rim polygons located in the center of the Dalangtan playa of the western Qaidam Basin. Our results suggest that the features of halite crustal floors and raised rims made by the accumulation of gypsum may be common in polygons developed under hyper-arid and highly evaporative conditions on both Earth and Mars.

2. Geological background

2.1. The Qaidam Basin

The Qaidam Basin is surrounded by the Qilian, Kunlun, and Altyn-Tagh Mountains, and forms an intermontane basin with a nearly rhombic outline (Fig. 1). The formation of the Qaidam Basin began when the Indian Plate collided with the Eurasian Continental Plate during the Mesozoic. During the Paleocene, a mega-lake likely formed in the western Qaidam Basin (Rieser et al., 2009) when the elevation of the basin was still low and the surrounding mountain ranges did not block moist air, allowing for a somewhat humid climate. During the Eocene, the center of the mega-lake began to migrate from west to east after the collision of the Indian subcontinent with Eurasia, and the basin became endorheic (Yin et al., 2008). Although the elevation of the Altyn-Tagh and Qilian Mountains increased from the late Oligocene to Miocene (Wang et al., 1999), the overall climate remained relatively humid and provided sufficient water to sustain a mega-lake with an estimated area of 4.8×10^5 km^2 (Huang and Han, 2007; Wang et al., 1999; Zhang, 1987). From the Miocene to the Pliocene, Himalayas Movement caused uplift of the entire Qinghai–Tibet Plateau, including the Qaidam Basin, significantly blocking the passage of moisture over the surrounding mountains (Han et al., 2014) and accelerating aridity in the basin (Wang et al., 1999). The resulting arid climate caused the paleo-lakes in the western basin to shrink into playas through evaporation. Two major episodes of salt deposition were recorded in the Qaidam Basin (Chen and Bowler, 1986; Wang et al., 1999; Yin et al., 2008), which were followed by the development of ubiquitous wind-sculpted landforms on the basin floor, such as polygons, gullies, alluvial fans, sand dunes, and yardangs (Anglés and Li, 2017; Xiao et al., 2017).

2.2. The study area

The study area is located in Dalangtan Playa, approximately 75 km south of the Altyn-Tagh Mountains (Fig. 1; Cheng et al., 2021; Dang et al., 2018). The terrain with pan-like polygons is adjacent to the JPPs terrain reported by Cheng et al. (2021). No perennial river water recharges the Dalangtan Playa, the dry salt flats 44 km long and 6–15 km wide that cover an area of ~500 km^2 (Huang and Han, 2007; Zhang, 1987). The local meteorological station recorded data on air temperature, precipitation, and evaporation in Dalangtan Playa from 1980 to 2011 (Kong et al., 2013). The mean annual temperature is 3.5 °C, with mean temperatures of −13 °C and 16 °C in January and July,

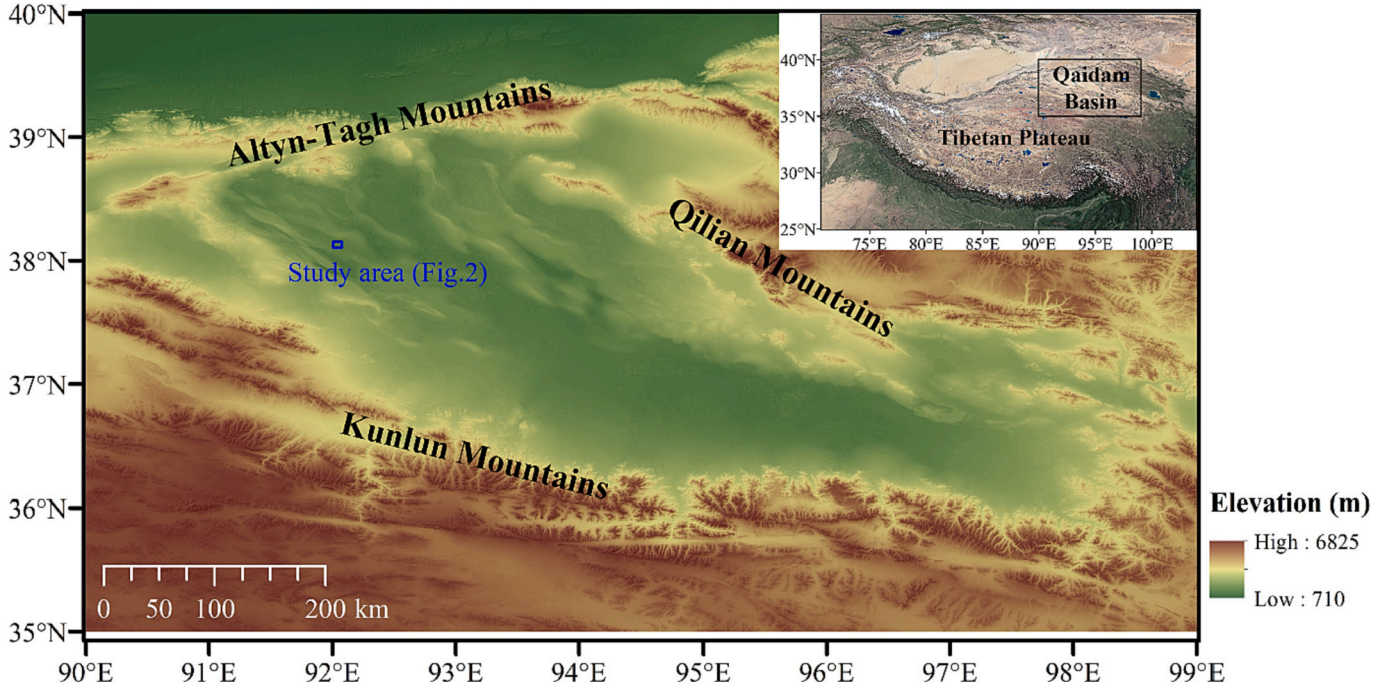

Fig. 1. Topographic map of the Qaidam Basin. The location of the terrain with pan-like polygons is marked with a blue box. The inset in the upper-right corner shows the location of the Qaidam Basin on the Qinghai–Tibet Plateau.

respectively; mean annual precipitation is 51 mm, and mean annual evaporation is >2590 mm (Kong et al., 2013). In the western basin, the mean annual precipitation is <20 mm (Han et al., 2014).

3. Methodology

3.1. Morphological mapping

The morphological characteristics of the terrain and the selected sampling sites are shown in Fig. 2. The topographic parameters of the polygons (e.g., size and shape) were measured on a high-resolution (~0.5 m/pixel) map extracted from WorldView-2 of Google Earth. Fig. 2 also compares polygons in Area A, which have complete rims, with those in Area B, which have incomplete rims. High-resolution aerial photographs of the site were taken using a DJI Phantom 4rtk drone. The aerial photographs were processed with photogrammetric software (ContextCapture) to create a high-resolution (~0.2 m/pixel) digital elevation model (DEM) of the region (Fig. 3; Li et al., 2022). This DEM was used for further analysis of polygonal features.

3.2. Field survey, sample acquisition, and analysis

Sampling sites in the study area were located in two areas with different morphological characteristics. Material from the surface and subsurface (approximate depth of 30 cm) was collected from the center to the rim at 6-m intervals to assess vertical variations, surface weathering, and the mechanism of rim formation (Fig. 4). We collected samples from three polygons with complete rims in Area A and one polygon with incomplete rims in Area B. Samples were sealed in ziplock bags until laboratory analysis.

All samples were subjected to powder X-ray diffraction (XRD) for qualitative identification and semi-quantitative analysis of mineralogical composition using an X-ray diffractometer (Japan Rigaku SmartLab) with Cu-Kα radiation ($\lambda = 0.154056$ nm) at 40 kV/Ma. The 2θ values were scanned from 3° to 80° with a scan rate of 20° per minute and a step of 0.02° at the University of Science and Technology of China. Jade 6.5 software was used to qualitatively and quantitatively process the mineral composition data.

4. Observations

4.1. Morphology of the pan-like polygons

The terrain with the pan-like polygons is about 3 km^2 (Fig. 2). These polygons have a similar appearance but are irregularly connected in a spatial network. The polygons in the northeastern part of the study area have complete rims, while the polygons in the southwest have incomplete rims (Fig. 3). The polygons in Area A have a lower topography of ~5 m than Area B (Fig. 3). These polygons are mainly between 60 and 120 m in size (Fig. 5) and are evenly distributed in space. In Area A, the width of the raised rims ranges from ~10 to 30 m and the height of the rim ranges from ~0.8 to 2.1 m. In Area B, the width of the raised rims ranges from ~0 to 20 m, and the height ranges from ~0 to 1.4 m. The generally smaller widths and heights of the polygonal rims in Area B than those in Area A are due to the incomplete nature of the rims in Area B (Fig. 3). Overall, the rims of the polygons are fully developed and form complete contours in the northeast, while they are incomplete in the southwest.

4.2. Mineral composition of the polygonal terrain

Our field observations showed that the polygonal surface contained gypsum crystals, that were particularly rich at the rims (Fig. 4). The gypsum crystals were mostly prismatic or lenticular and only a few centimeters in size, indicating an evaporative depositional environment in the paleo-lake (Magee, 1991).

XRD results (Fig. 7) showed the distribution of mineral compositions (Fig. 6) of the sampled surface and subsurface materials from the center to the rim of polygons P1, P3, and P4 in Area A, and P2 in Area B. The XRD patterns (Fig. 6) showed that gypsum content was higher in the surface samples than in the subsurface, but halite content was consistently higher in the subsurface samples than in the surface samples. In all polygons measured, gypsum and halite contents varied considerably between the surface and subsurface samples, whereas illite and other mineral contents varied less (Fig. 6 and Table A1). Surface samples consistently contained high amounts of gypsum (mainly >20 wt%), considerable amounts of quartz (~15 wt%), and small amounts of other minerals, such as clinochlore, calcite, aragonite, and halite (~2 wt%). The subsurface mineral compositions had high amounts of halite

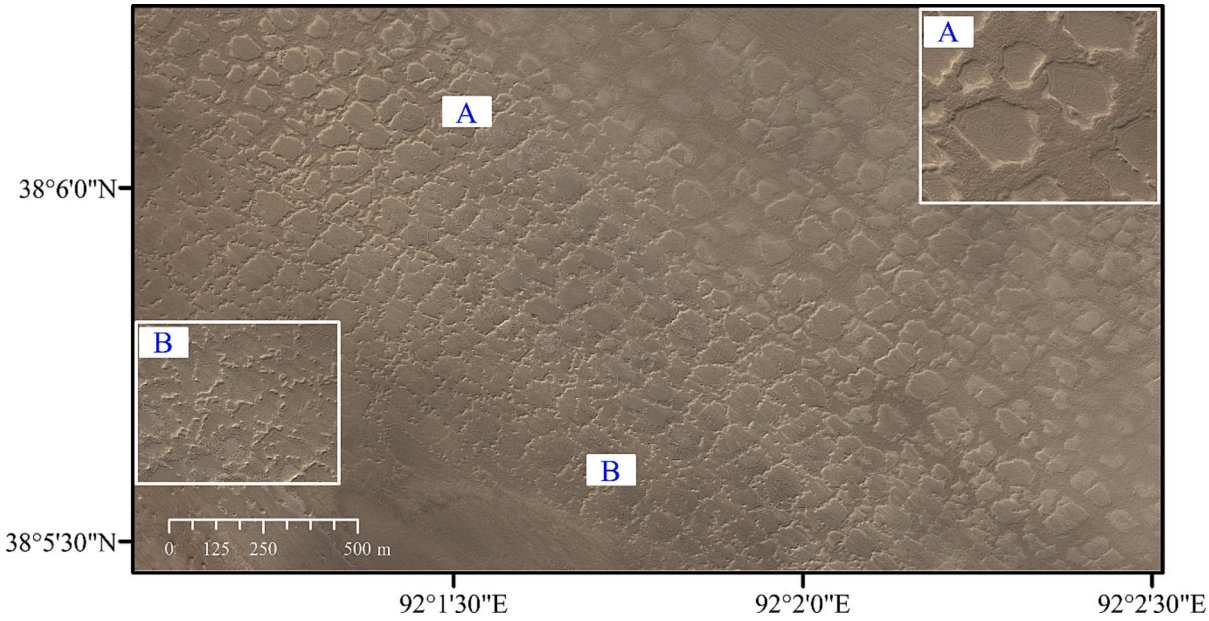

Fig. 2. Satellite image showing the study area, which contains a network of pan-like polygons. The white rectangles labeled A and B show the different features in polygonal rim between the areas labeled A and B. The polygons in Area A have complete rims, while those in Area B have incomplete rims.

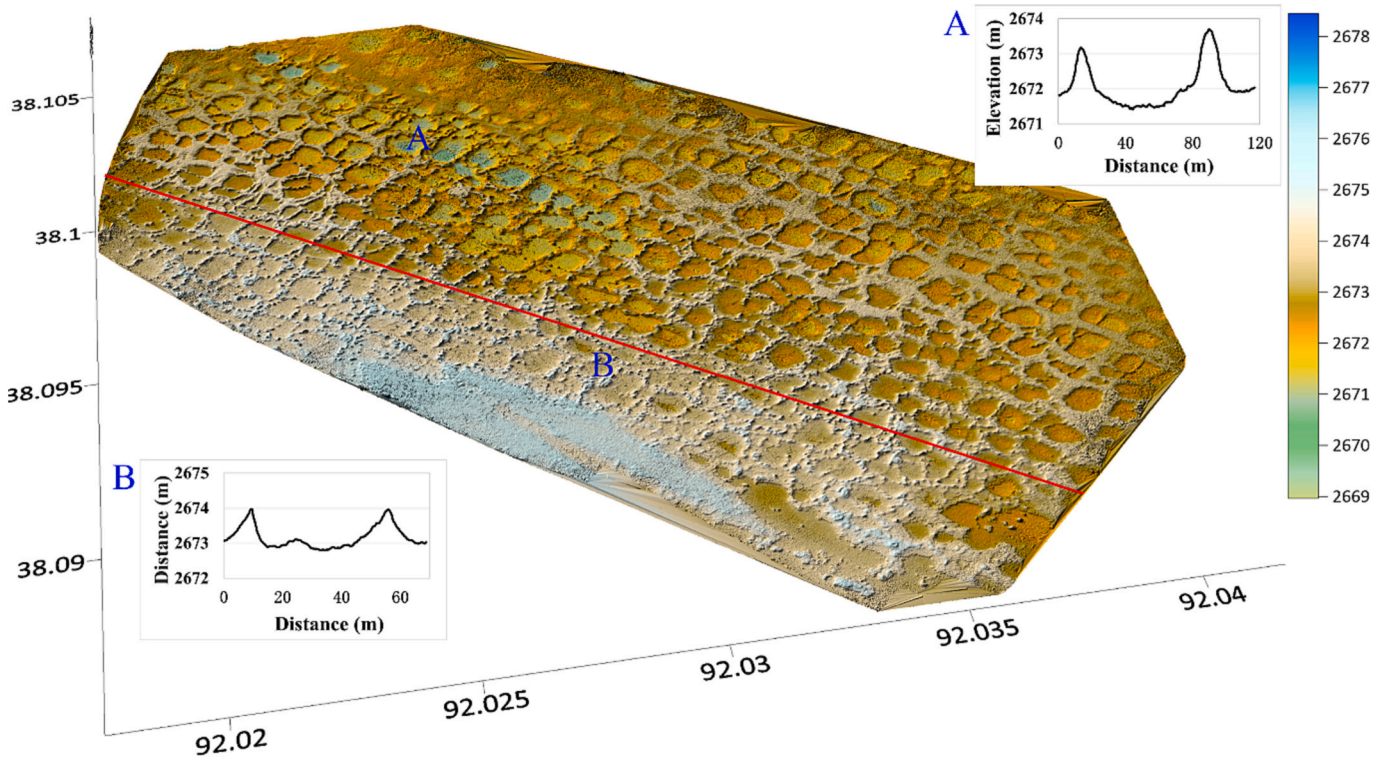

Fig. 3. Digital elevation model (DEM) of the study area generated by uncrewed aerial vehicle survey. The red demarcation line between Area A and Area B. The insets show cross-sections of the polygons in areas A and B. Both types of polygons contain raised rims, but those in Area A have higher rims.

(mainly >20 wt%), as shown in Fig. 7 and Tables A1, A2, A3, and A4.

In all surface samples, gypsum contents were consistently higher at the rims than at the floor of the polygons (Fig. 4), whereas no significant difference was observed for the other minerals (Fig. 7 and Table A1). In the subsurface samples, halite and gypsum contents were consistently higher at the rims than at the floor of the polygons, while no significant difference was observed for the other minerals (Fig. A1).

Subsurface samples from the polygonal rims in Area B contained a higher proportion of halite and a lower proportion of gypsum than those in Area A, while there was no significant difference in the center area (Fig. 7). Surface samples in Area B contained a relatively lower proportion of gypsum than those in Area A in general, while there were no significant differences in the other minerals (Tables A1, A2, A3, and A4).

5. Interpretation and discussion

5.1. Genesis of the pan-like polygons

Polygons with different characteristics may originate from different geologic contexts. For example, thermal contraction in permafrost forms cracks and gradually shapes vertical ice wedges with seasonal freeze-thaw cycles (Lachenbruch, 1962); polygonal features with a desiccation origin can be found in playa environments (Dang et al., 2018; Neal et al., 1968); polygonal fractures in lava flows are due to lava cooling (Aydin and DeGraff, 1988; Peck and Minakami, 1968). Given the playa context and the high ratio of evaporation to precipitation in the western Qaidam Basin, desiccation is the most likely formation mechanism. The spatial transformation of the characteristics of these pan-like polygons is consistent with the observed spatial change in mineral composition. We propose a conceptual model (Fig. 8) that includes the formation of a halite crust at the polygonal floors and the accumulation of gypsum at the polygon boundaries that raises and widens the rims.

Mineralogically, the surface samples contain aeolian deposits of quartz particles. Illite and chlorite are non-expansible 2:1 clays that do not contribute to the formation and accretion of the raised polygonal rims. Illite content was high at all four sampled sites, but, without a significant change, suggesting that it plays an insignificant role in the formation of the raised rims. The formation of the raised rims can be explained by the change in the proportions of gypsum and halite from the center to the rim of these pan-like polygons. As we observed, the subsurface of the polygonal center is composed of a thick halite crust, while the rims are composed of highly accumulated gypsum (Figs. 4b and 7), which can be attributed to the evaporative deposition of pore fluids from the subsurface (Fig. 8).

The mineralogical changes observed in the samples from the terrain of the pan-like polygons can be explained by a long-term process that begins with the drying of the lacustrine brine and the subsequent migration of the subsurface pore fluids when the climate becomes arid. In the initial phase, the lacustrine brine contained various ions in solution, including Na^+, Ca^{2+}, Cl^-, and SO_4^{2-} (Fig. 8). In the Qaidam Basin, a transition from a relatively humid to a drier climate occurred during the recent prolonged drought (Chen and Bowler, 1986), resulting in desiccation and triggering polygonal cracks in the lake sediments (Dang et al., 2018). The mineral compositions of the four sampled sites consistently show that evaporation of the lake brine in the middle phase leads to the formation of a halite crust that diverts the pore fluids with high Ca^{2+} content to the polygonal rims, which deposit to form gypsum at the polygonal rims, and eventually form a new horizon above the polygonal floor (Figs. 4 and 8; Krinsley, 1970; Lasser et al., 2023; Ye et al., 2019). Because Area A is topographically lower than Area B, more subsurface fluids can flow into the former (Fig. 3). Accordingly, polygons in Area B have developed immaturely and have incompletely raised rims due to the lower influx of pore fluids. Sufficient subsurface pore fluid allows for a continuous process in which the developed polygon edges become higher and wider (Dang et al., 2018; Lasser et al., 2023). During the development phase, which is accompanied by heavy evaporation, the halite crust thickens, and additional gypsum is deposited on the polygon edges to raise and widen the polygon rims into wide belts between the polygons in Area A (Fig. 8; Li et al., 2010).

Dang et al. (2018) suggested that polygons with raised rims form due

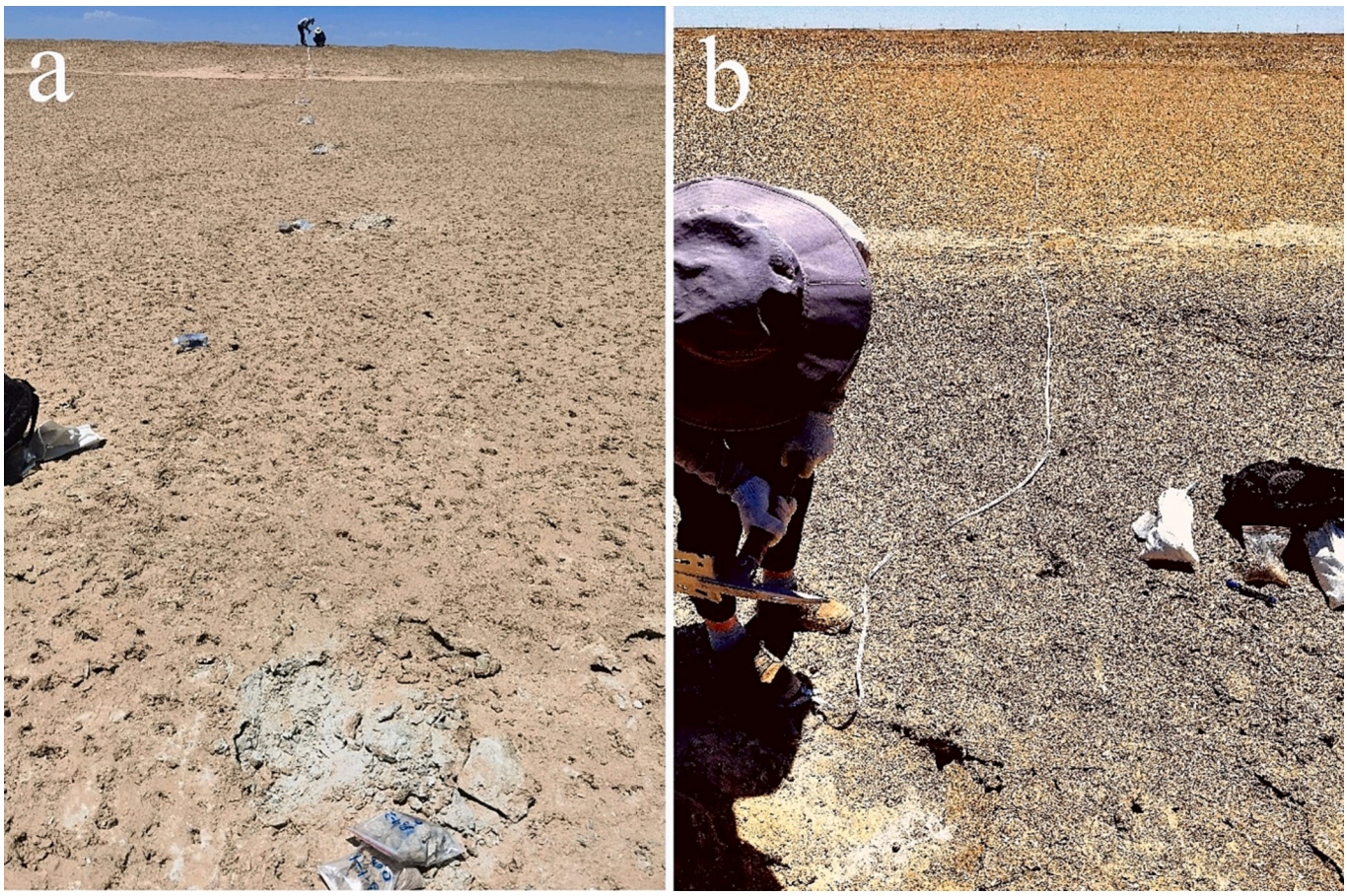

Fig. 4. Field images of the pan-like polygons. (a) The image was taken at the center of a polygon, showing the raised rim/boundary belt at the far side. (b) The image was taken on the rim/boundary belt of the polygon. Dense gypsum crystals piled at the polygonal rim/boundary belt show a light purple color.

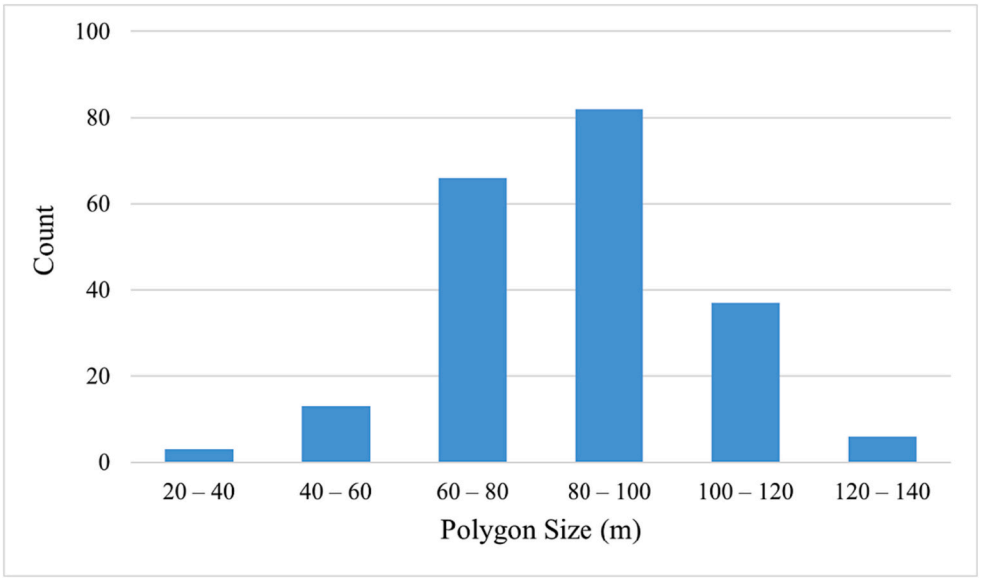

Fig. 5. Distribution of polygon sizes in the study area.

to evaporative halite growth, overlooking contributions from gypsum and spatial variations in mineral composition within each polygonal structure and throughout the polygonal network. Cheng et al. (2021) demonstrated that chemical conversion of sodium sulfate to calcium sulfate leads to the formation of the raised rims of JPPs, but the study ignored the role of the halite crust in controlling subsurface fluid migration. Tucker (1981) observed that the mineral composition (halite, anhydrite, detrital quartz, feldspar, and clay minerals) of the raised rims was similar to those of our study. Tucker (1981) suggested that secondary halite deposition and the filling of clastic material in fractures

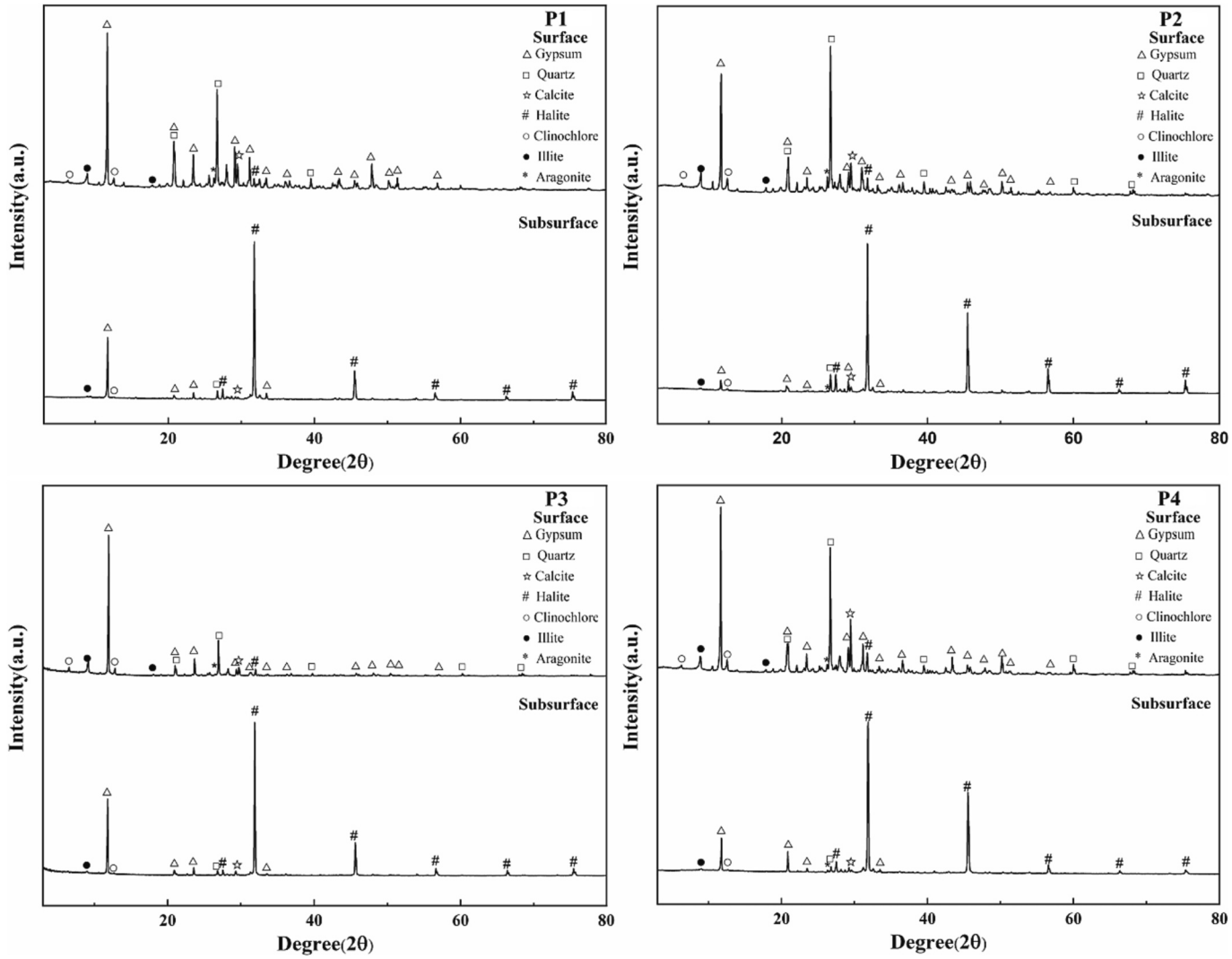

Fig. 6. The XRD measured mineralogical compositions of the surface and subsurface samples of the four studied polygons. The abundance of gypsum on the surface is consistently higher than the subsurface at the rim of polygons but the abundance of halite on the subsurface is higher than that on the surface in general.

result in raised rims, but does not show the change in mineral composition, although aeolian deposits may indeed be preserved by a raised gypsum rim, as we observed in this study (Fig. 4b). Wang et al. (2023) found a polygonal surface containing gypsum at the Zhurong landing site, which could be due to contraction during groundwater evaporation or fracture of the indurated crust. Lasser et al. (2023) modeled the transport of upward diffusing pore fluids beneath the salt crust to the polygonal boundaries to produce the polygonal raised rim.

5.2. *Implications for the formation of polygon landforms on Mars*

Polygonal landforms are also commonly observed on Mars and have been studied in detail through comparisons with their analogs formed in arid climatic environments on Earth (Anglés and Li, 2017; Xiao et al., 2017). The observed polygons on Mars range in size from meters to kilometers and some of them have raised rim structures (Dang et al., 2020; El Maarry et al., 2013; Mangold, 2005; McGill and Hills, 1992). Topographic variations, water ice condition, temperature, wet-and-dry cycle, and saline activity have been suggested as possible factors in the formation of polygons on Mars (Dang et al., 2018). The formation of polygons on the floor of some crater basins is mainly due to the desiccation of lake sediments (El Maarry et al., 2010; Ye et al., 2019). The formation of medium and large polygons with raised rims is generally associated with the presence of saturated brine (Dang et al., 2018; Neal et al., 1968). However, most studies of polygonal landforms on Mars rely on remote sensing techniques thus information on the mineral composition and evolutionary dynamics of these features is lacking. Our study of such analogs provides an opportunity to reveal the temporal and spatial relationships between the salt crust (halite) and gypsum deposits at polygonal rims in arid climatic environments.

The pan-like polygons in the Qaidam Basin are analogous to the medium (10–100 m) and large (100–300 m) polygons with raised rims in the chloride-bearing and clay mineral terrain on Mars (Dang et al., 2018; Ye et al., 2019). Hundreds of polygonal terrains with chloride-bearing material and raised rims have been found in the southern highlands of Mars (Osterloo et al., 2010). The observed presence of chloride on Mars possibly indicates that groundwater was once active in these lacustrine environments on Mars. Due to limitations such as the resolution of hyperspectral images and lack of in situ data, sulfates such as gypsum are difficult to detect in the raised rims of the polygons. Desiccation is the most likely origin of the polygons on both Earth and playas on Mars (Dang et al., 2018; Neal et al., 1968). Our results suggest the uncoupled roles of halite and gypsum: Lacustrine brine in the early phase contributes to the halite crust, while gypsum is deposited to the raised rims of the polygons later in the phase with the evaporation of subsurface pore fluid (Goodall et al., 2000; Lasser et al., 2023). This

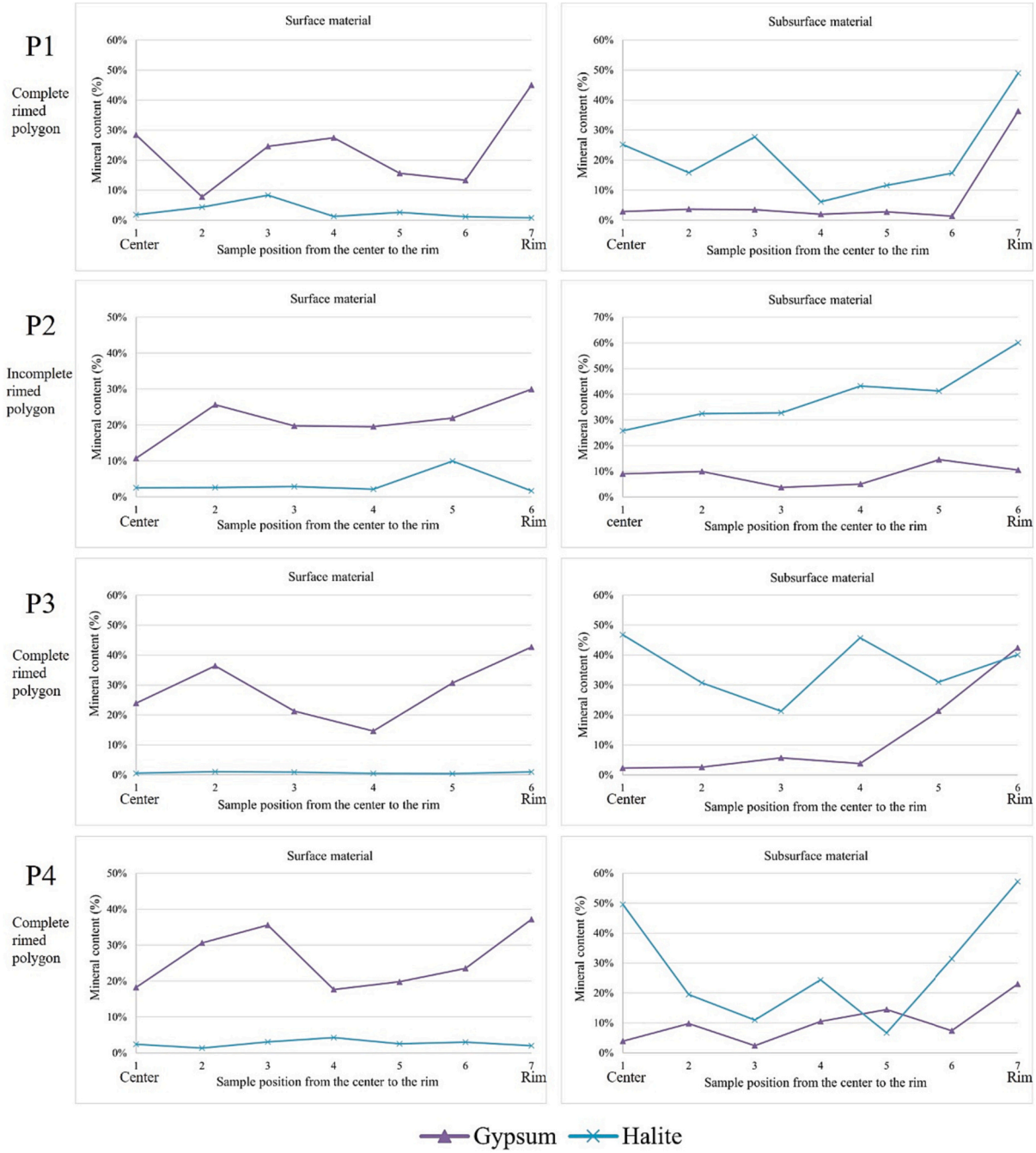

Fig. 7. Gypsum and halite contents in samples from center to rim of polygons in Area A (P1, P3, and P4) and Area B (P2), measured using powder XRD. P1 and P4 each contain seven sampling points, and P2 and P3 each contain six sampling points. The distance between two adjacent sampling points is ~6 m. All mineral contents in samples from centers to rims of polygons are shown in Fig. A1. Detailed compositions are listed in Tables A1, A2, A3, and A4.

alternative mechanism may explain the formation of medium- or large-sized polygons with raised rims on Mars. The rim widths of the medium polygons range from ~0.5 to 2 m. The rim widths of the large polygons are about 10 m (Fig. 9b) and even up to 20 m (Fig. 10c). Despite the lack of DTM from HiRISE images, the height of the rim is estimated to be within 1 m based on the shadow length and the angle of solar incidence. The height of the rim is up to 2 m in Fig. 10c. These polygons exhibit double rims (Figs. 9a-b) formed on chloride-rich terrain, an environment like the playa in the center of the western Qaidam Basin (inset of Fig. 9b). Medium and large polygons tend to lose their double rims due to further deposition of minerals and the filling and weathering of extraneous material (Fig. 10; Ye et al., 2019), which is consistent with our findings in the Qaidam Basin. It has been suggested that the formation of medium and large polygons with raised rims was associated with saturated brine (Neal et al., 1968). However, the inability of visible and near-infrared wavelength remote sensing imagery to penetrate the surface and the inadequacy of in-situ data hinder the interpretation of the formation of medium and large martian polygons with raised rims. We suggest that the polygons with raised rims observed on Mars have similar lateral and vertical structures caused by the strong evaporation of subsurface fluids and that their structural evolution stopped at an early stage due to a limited supply of subsurface fluids. Therefore, polygonal terrains with chloride-bearing material are potential analogs on Mars and should be looked for by future orbital, airborne, or landed assets.

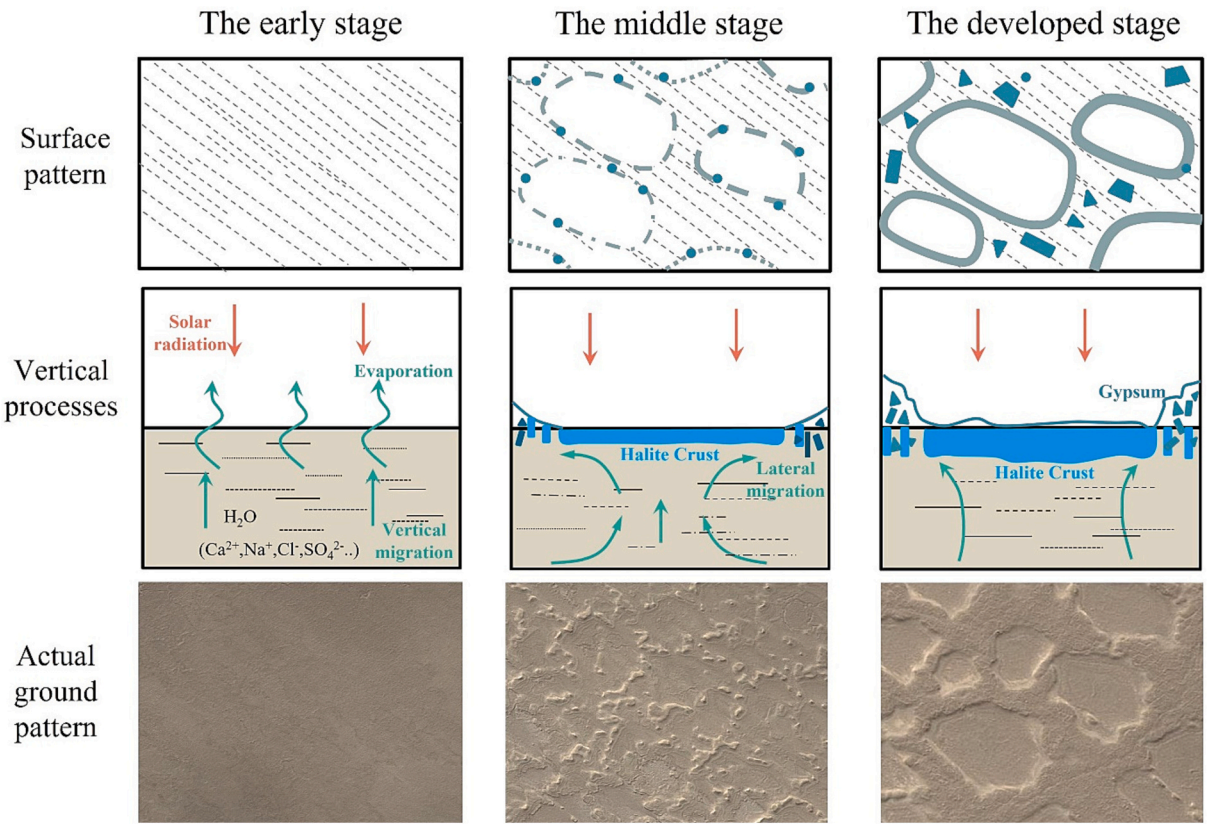

Fig. 8. Schematic representations of the formation of the raised rims/boundary belts of the pan-like polygons in the Qaidam Basin. The early stage is characterized by the drying of lacustrine (left column). Continued evaporation causes the surface to dry out and form polygonal cracks. In the middle stage, the halite crust begins to form and diverts the evaporative fluids, and gypsum begins to accumulate at the rim (middle column). In the development stage, the halite crust thickens, and more gypsum is deposited to widen the polygonal rims into wide belts (right column).

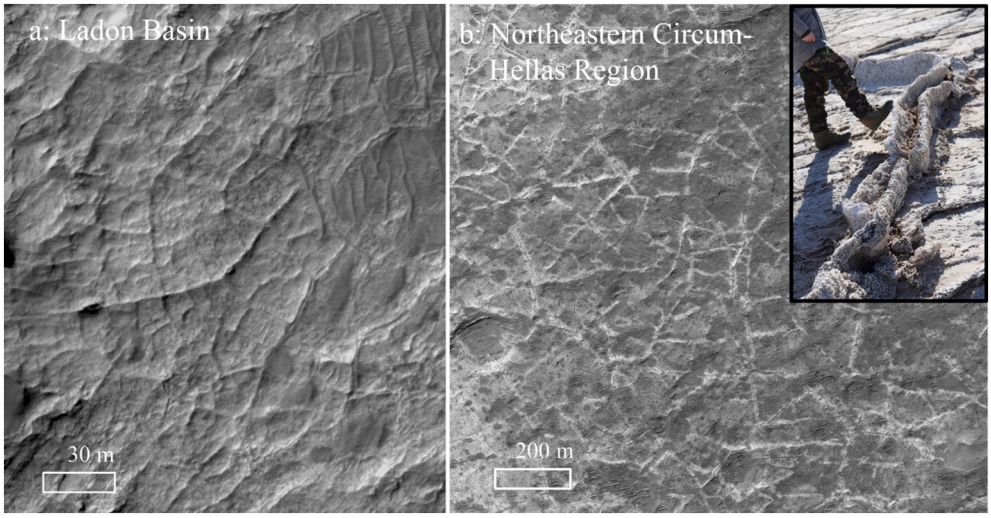

Fig. 9. Observations of polygons with double raised rims on Mars. (a) Medium-sized polygons on a chloride-bearing terrain in the Ladon Basin (HiRISE image ID: PSP_008720_1610). (b) Large-sized polygons on a chloride-bearing terrain in the northeastern Circum-Hellas region (HiRISE image ID: ESP_024922_1570). The inset shows a double rim feature observed in a playa field in the center of the western Qaidam Basin.

6. Conclusions

We have observed pan-like polygons in the playas of the western Qaidam Basin and described spatial variations in structure and mineral composition within each polygon and throughout the study area. We conducted morphological and mineralogical analyses using remote sensing, in-situ field investigations, and laboratory analyses to uncover a possible mechanism for the formation of the polygons. Here are our findings:

1) The pan-like polygons (~60–120 m) are irregular in shape and outlined by raised rims or boundary belts up to 30 m wide. The polygons in the northeastern part of the terrain have complete raised

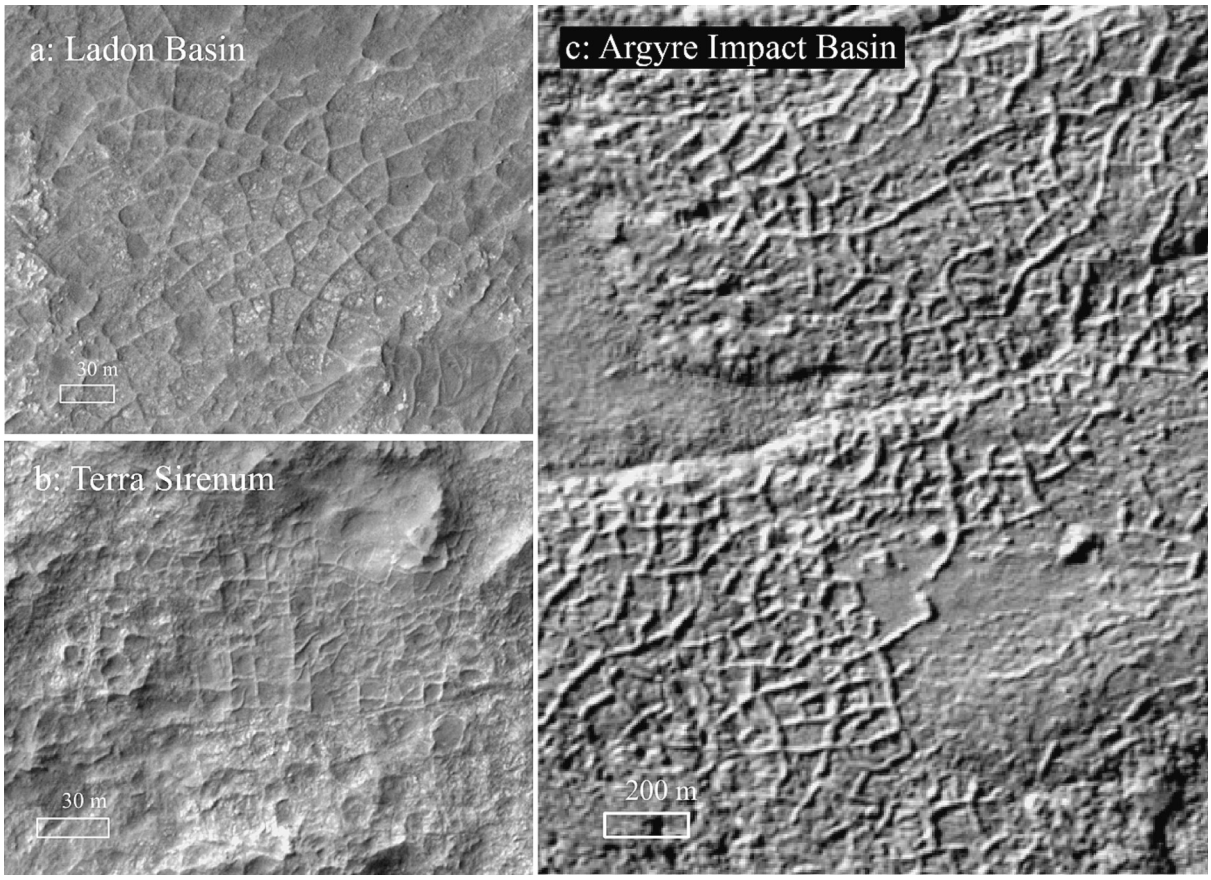

Fig. 10. Observations of polygons with fully developed raised rims on Mars. (a) Medium-sized polygons on a chloride-bearing terrain in the Ladon Basin (HiRISE image ID: ESP_047343_1610). (b) Medium-sized polygons on a chloride-bearing terrain in the Terra Sirenum (HiRISE image ID: PSP_010387_1485). (c) Large-sized polygons in the Argyre Impact Basin (CTX image ID: B01_009907_1433).

rims, while those in the southwestern part have incomplete raised rims.

2) The surface of the polygons has consistently higher gypsum than halite contents and shows an accumulation of gypsum at the rim of the polygons. The feature of halite content in the subsurface is much higher than on the surface, which forms the halite salt crust. There are no obvious differences or features in the other minerals.
3) The polygonal floors consistently have a salt crust, throughout, consisting mainly of halite in the subsurface deposited by drying of the salt lakes, and the polygonal raised rims consist of gypsum deposited from the subsurface pore fluid after the formation of the salt crust.
4) The formation of halite crusts and gypsum-raised rims is a ubiquitous process in the formation of medium to large polygons in an arid environment, which could also provide new insights into the formation of the analogous polygons on Mars.

Declaration of competing interest

The authors declare that they have no known competing financial interests or personal relationships that could have appeared to influence the work reported in this paper.

Data availability statement

The HiRISE and CTX images in the paper are available in the NASA Planetary Data System (https://pds.jpl.nasa.gov/). The topographic map is available in the NASA Earth Data System (https://www.earthdata.nasa.gov/).

Acknowledgments

We thank the editor and two anonymous reviewers and Professor Joseph Levy for their very constructive comments, suggestions, and discussions. This work was supported by grants from the Research Grants Council of Hong Kong (RIF Project No: R5043-19, Project No: PolyU 15210520).

Appendix A. Supplementary data

Supplementary data to this article can be found online at https://doi.org/10.1016/j.geomorph.2023.108934.

References

Anglés, A., Li, Y., 2017. The western Qaidam Basin as a potential Martian environmental analogue: an overview. J. Geophys. Res.: Planets 122 (5), 856–888.
Aydin, A., DeGraff, J.M., 1988. Evolution of polygonal fracture patterns in lava flows. Science 239 (4839), 471–476.
Chen, K., Bowler, J., 1986. Late Pleistocene evolution of salt lakes in the Qaidam basin, Qinghai province, China. Palaeogeogr. Palaeoclimatol. Palaeoecol. 54 (1–4), 87–104.
Cheng, Z., Xiao, L., Wang, H., Yang, H., Li, J., Huang, T., Xu, Y., Ma, N., 2017. Bacterial and archaeal lipids recovered from subsurface evaporites of Dalangtan Playa on the Tibetan Plateau and their astrobiological implications. Astrobiology 17 (11), 1112–1122.
Cheng, R.-L., He, H., Michalski, J.R., Li, Y.-L., 2021. A new type of polygonal terrain formed by sulfate weathering in arid regions. Geomorphology 383, 107695.
Dang, Y., Xiao, L., Xu, Y., Zhang, F., Huang, J., Wang, J., Zhao, J., Komatsu, G., Yue, Z., 2018. The polygonal surface structures in the Dalangtan Playa, Qaidam Basin, NW China: controlling factors for their formation and implications for analogous Martian landforms. J. Geophys. Res.: Planets 123 (7), 1910–1933.

Dang, Y., Zhang, F., Zhao, J., Wang, J., Xu, Y., Huang, T., Xiao, L., 2020. Diverse polygonal patterned grounds in the Northern Eridania Basin, Mars: possible origins and implications. J. Geophys. Res.: Planets 125 (12), e2020JE006647.
El Maarry, M.R., Markiewicz, W., Mellon, M., Goetz, W., Dohm, J., Pack, A., 2010. Crater floor polygons: desiccation patterns of ancient lakes on Mars? J. Geophys. Res.: Planets 115 (E10).
El Maarry, M.R., Pommerol, A., Thomas, N., 2013. Analysis of polygonal cracking patterns in chloride-bearing terrains on Mars: indicators of ancient playa settings. J. Geophys. Res.: Planets 118 (11), 2263–2278.
El-Maarry, M.R., Watters, W., Yoldi, Z., Pommerol, A., Fischer, D., Eggenberger, U., Thomas, N., 2015. Field investigation of dried lakes in western United States as an analogue to desiccation fractures on Mars. J. Geophys. Res.: Planets 120 (12), 2241–2257.
Goodall, T.M., North, C.P., Glennie, K.W., 2000. Surface and subsurface sedimentary structures produced by salt crusts. Sedimentology 47 (1), 99–118.
Han, W., Fang, X., Ye, C., Teng, X., Zhang, T., 2014. Tibet forcing Quaternary stepwise enhancement of westerly jet and central Asian aridification: carbonate isotope records from deep drilling in the Qaidam salt playa, NE Tibet. Glob. Planet. Chang. 116, 68–75.
Huang, Q., Han, F., 2007. Evolution of Salt Lakes and Palaeoclimate Fluctuation in Qaidam Basin. Science Press, Beijing, China.
Kapp, P., Pelletier, J.D., Rohrmann, A., Heermance, R., Russell, J., Ding, L., 2011. Wind erosion in the Qaidam basin, Central Asia: implications for tectonics, paleoclimate, and the source of the Loess Plateau. GSA Today 21 (4/5), 4–10.
Kong, F., Kong, W., Hu, B., Zheng, M., 2013. Meterological data, surface temperature and moisture conditions at the Dalantan Mars Analogous Site. In: Qinghaitibet Plateau, China. 44th Annual Lunar and Planetary Science Conference, Woodlands, Texas, No. 1719, p. 1743.
Kong, W., Zheng, M., Kong, F., Chen, W., 2014. Sulfate-bearing deposits at Dalangtan Playa and their implication for the formation and preservation of martian salts. Am. Mineral. 99 (2–3), 283–290.
Kong, F., Zheng, M., Hu, B., Wang, A., Ma, N., Sobron, P., 2018. Dalangtan Saline Playa in a hyperarid region on Tibet Plateau: I. Evolution and environments. Astrobiology 18 (10), 1243–1253.
Krinsley, D.B., 1970. A Geomorphological and Paleoclimatological Study of the Playas of Iran: Part II. Geological Survey United States Department of the Interior, Washington DC, USA.
Lachenbruch, A.H., 1962. Mechanics of Thermal Contraction Cracks and Ice-Wedge Polygons in Permafrost, Vol. 70. Geological Society of America.
Lasser, J., Nield, J.M., Ernst, M., Karius, V., Wiggs, G.F., Threadgold, M.R., Beaume, C., Goehring, L., 2023. Salt polygons and porous media convection. Phys. Rev. X 13 (1), 011025.
Li, M., Fang, X., Yi, C., Gao, S., Zhang, W., Galy, A., 2010. Evaporite minerals and geochemistry of the upper 400 m sediments in a core from the Western Qaidam Basin, Tibet. Quat. Int. 218 (1–2), 176–189.
Li, Z., Wu, B., Liu, W.C., Chen, Z., 2022. Integrated photogrammetric and photoclinometric processing of multiple HRSC images for pixelwise 3-D mapping on Mars. In: IEEE Transactions on Geoscience and Remote Sensing, 60, pp. 1–13. https://doi.org/10.1109/TGRS.2021.3106737.
Lokier, S., 2012. Development and evolution of subaerial halite crust morphologies in a coastal sabkha setting. J. Arid Environ. 79, 32–47.
Magee, J., 1991. Late Quaternary lacustrine, groundwater, aeolian and pedogenic gypsum in the Prungle Lakes, southeastern Australia. Palaeogeogr. Palaeoclimatol. Palaeoecol. 84 (1–4), 3–42.
Mangold, N., 2005. High latitude patterned grounds on Mars: classification, distribution and climatic control. Icarus 174 (2), 336–359.
Marchant, D.R., Head III, J.W., 2007. Antarctic dry valleys: Microclimate zonation, variable geomorphic processes, and implications for assessing climate change on Mars. Icarus 192 (1), 187–222.
Marchant, D., Lewis, A.R., Phillips, W.M., Moore, E., Souchez, R., Denton, G.H., Sugden, D., Potter Jr., N., Landis, G.P., 2002. Formation of patterned ground and sublimation till over Miocene glacier ice in Beacon Valley, southern Victoria Land, Antarctica. Geol. Soc. Am. Bull. 114 (6), 718–730.
McGill, G.E., Hills, L.S., 1992. Origin of giant Martian polygons. J. Geophys. Res.: Planets 97 (E2), 2633–2647.
Meyer, B., Tapponnier, P., Bourjot, L., Metivier, F., Gaudemer, Y., Peltzer, G., Shunmin, G., Zhitai, C., 1998. Crustal thickening in Gansu-Qinghai, lithospheric mantle subduction, and oblique, strike-slip controlled growth of the Tibet plateau. Geophys. J. Int. 135 (1), 1–47.
Neal, J.T., Langer, A.M., Kerr, P.F., 1968. Giant desiccation polygons of Great Basin playas. Geol. Soc. Am. Bull. 79 (1), 69–90.
Osterloo, M.M., Anderson, F.S., Hamilton, V.E., Hynek, B.M., 2010. Geologic context of proposed chloride-bearing materials on Mars. J. Geophys. Res.: Planets 115 (E10).
Pechmann, J.C., 1980. The origin of polygonal troughs on the northern plains of Mars. Icarus 42 (2), 185–210.
Peck, D.L., Minakami, T., 1968. The formation of columnar joints in the upper part of Kilauean lava lakes, Hawaii. Geol. Soc. Am. Bull. 79 (9), 1151–1166.
Rieser, A.B., Bojar, A.-V., Neubauer, F., Genser, J., Liu, Y., Ge, X.-H., Friedl, G., 2009. Monitoring Cenozoic climate evolution of northeastern Tibet: stable isotope constraints from the western Qaidam Basin, China. Int. J. Earth Sci. 98 (5), 1063–1075.
Tucker, R.M., 1981. Giant polygons in the Triassic salt of Cheshire, England; a thermal contraction model for their origin. J. Sediment. Res. 51 (3), 779–786.
Wang, J., Wang, Y.J., Liu, Z.C., Li, J.Q., Xi, P., 1999. Cenozoic environmental evolution of the Qaidam Basin and its implications for the uplift of the Tibetan Plateau and the drying of Central Asia. Palaeogeogr. Palaeoclimatol. Palaeoecol. 152 (1–2), 37–47.
Wang, J., Zhao, J., Xiao, L., Peng, S., Zhang, L., Zhang, Z., Gao, A., Qiao, H., Wang, L., Zhang, S., 2023. Recent aqueous activity on Mars evidenced by transverse aeolian ridges in the Zhurong exploration region of Utopia Planitia. Geophys. Res. Lett. 50 (6), e2022GL101650.
Weinberger, R., 1999. Initiation and growth of cracks during desiccation of stratified muddy sediments. J. Struct. Geol. 21 (4), 379–386.
Xiao, L., Wang, J., Dang, Y., Cheng, Z., Huang, T., Zhao, J., Xu, Y., Huang, J., Xiao, Z., Komatsu, G., 2017. A new terrestrial analogue site for Mars research: the Qaidam Basin, Tibetan Plateau (NW China). Earth Sci. Rev. 164, 84–101.
Ye, B., Huang, J., Michalski, J., Xiao, L., 2019. Geomorphologic characteristics of polygonal features on chloride-bearing deposits on Mars: Implications for martian hydrology and astrobiology. J. Earth Sci. 30, 1049–1058.
Yin, A., Dang, Y.-Q., Zhang, M., Chen, X.-H., McRivette, M.W., 2008. Cenozoic tectonic evolution of the Qaidam basin and its surrounding regions (part 3): structural geology, sedimentation, and regional tectonic reconstruction. Geol. Soc. Am. Bull. 120 (7–8), 847–876.
Zhang, P., 1987. Salt Lakes in Qaidam Basin. Science Press, Beijing, China.